

S100A4 Elevation Empowers Expression of Metastasis Effector Molecules in Human Breast Cancer

Thamir M. Ismail, Daimark Bennett, Angela M. Platt-Higgins, Morteta Al-Medhity,
Roger Barraclough, and Philip S. Rudland

Abstract

Many human glandular cancers metastasize along nerve tracts, but the mechanisms involved are generally poorly understood. The calcium-binding protein S100A4 is expressed at elevated levels in human cancers where it has been linked to increased invasion and metastasis. Here we report genetic studies in a *Drosophila* model to define S100A4 effector functions that mediate metastatic dissemination of mutant Ras-induced tumors in the developing nervous system. In flies overexpressing mutant Ras^{Val12} and S100A4, there was a significant increase in activation of the stress kinase JNK and production of the matrix metalloproteinase MMP1. Genetic or chemical blockades of JNK and MMP1 suppressed metastatic dissemination associated with

S100A4 elevation, defining required signaling pathway(s) for S100A4 in this setting. In clinical specimens of human breast cancer, elevated levels of the mammalian paralogs MMP2, MMP9, and MMP13 are associated with a 4- to 9-fold relative decrease in patient survival. In individual tumors, levels of MMP2 and MMP13 correlated more closely with levels of S100A4, whereas MMP9 levels correlated more closely with the S100 family member S100P. Overall, our results suggest the existence of evolutionarily conserved pathways used by S100A4 to promote metastatic dissemination, with potential prognostic and therapeutic implications for metastasis by cancers that preferentially exploit nerve tract migration routes. *Cancer Res*; 1–12. ©2016 AACR.

Introduction

Certain tumor cells have a propensity to invade the neighboring tissue and eventually establish new secondary tumors or metastases while others cannot (1, 2). These results suggest that a specific set of genes, different from those involved in the production of the neoplasia, are involved in promoting a complex series of steps to form metastases (3). The protein products of such genes have been termed metastasis-inducing proteins (MIP). One such gene/protein is S100A4 (4), a member of the S100-calcium-binding protein family (5). Although S100A4 cannot promote tumor formation directly, it can stimulate the remaining steps in the metastatic cascade in model rodent systems by combining with oncogenes such as Ras^{Val12} and *neu* (4, 6). Moreover, S100A4 is overexpressed in human primary tumors and is associated with the premature death of patients with different types of metastatic carcinomas, including those from the breast (7), oral mucosa, bladder, pancreas, prostate, colorectum, esophagus, lung, stomach, and thyroid glands (8). The elevation of S100A4 can trigger multiple biological functions, including cell migration, invasion, extracellular matrix remodeling, and angiogenesis (8, 9). How-

ever, it is unknown what are the biologically relevant molecular events from the plethora triggered by S100A4 in cultured mammalian cells (10). To generate a genetically tractable experimental model to investigate the molecular events triggered by S100A4, we have for the first time expressed human S100A4 in the fruit fly, *Drosophila melanogaster* by targeting its expression to the developing eye lobes (11) and not elsewhere in the brain or CNS (12, 13). *Drosophila* has conserved signal transduction pathways for cell cycle, growth control, and cell-to-cell communication (14) and a larval phase of only a few days, which can be interrogated by inhibitory chemicals applied directly to the growth medium. In addition, 70% of human cancer genes are conserved in the *Drosophila* model, but importantly none of the S100 family proteins are present (15). Overexpression of oncogenic Ras (Ras^{Val12}) causes the formation of tumors in the epithelial tissues of *Drosophila* (16), and these can be transformed into a malignant phenotype by disruption of suppressor genes such as *scribble* (*scrib*) and *lethal2* (17). In this new model we have for the first time generated transgenic flies capable of conditionally-expressing the open-reading frame of human S100A4 under GAL4/UAS-control (18). We show, after multiple crosses, that the S100A4 gene is required to disseminate Ras^{Val12} tumor cells from the optic lobes to the ventral nerve cord (VNC) and further afield in fly larvae. The combination of Ras^{Val12} and loss of *scrib* in *Drosophila* activates the JNK pathway and this activation induces the matrix metalloproteinase MMP1 to allow dissemination of the cancer cells in the Ras oncogenic system (16). Therefore, we have assessed whether c-Jun and *Drosophila* MMP1 are downstream targets for promoting dissemination in our Ras^{Val12}/S100A4 novel larval model using fly genetics and inhibitory chemicals, and whether there is a uniquely similar association between S100A4 and mammalian MMPs in human breast cancer.

Department of Biochemistry, Institute of Integrative Biology, University of Liverpool, Liverpool, United Kingdom.

Note: Supplementary data for this article are available at Cancer Research Online (<http://cancerres.aacrjournals.org/>).

Corresponding Author: Philip S. Rudland, University of Liverpool, Crown Street, Liverpool, Merseyside L69 7ZB, United Kingdom. Phone: 4415-1795-4474; Fax: 4415-1795-4408; E-mail: rudland@liverpool.ac.uk

doi: 10.1158/0008-5472.CAN-16-1802

©2016 American Association for Cancer Research.

89 Materials and Methods

90 Expression of S100A4 in *Drosophila melanogaster*

91 Human *S100A4* wild-type (*S100A4wt*; ref. 19) and inactive
92 mutant *S100A4Δ2* (20) were cloned and expressed in transgenic
93 flies as described in Supplementary Methods. Stable transgenic
94 lines were checked for *S100A4* expression by crossing with *da-*
95 *GAL4* flies (18) and Western blotted. Resultant *S100A4wt* and
96 *S100A4Δ2* progeny produced (mean ± SE) similar 7.7 ± 0.6 ng
97 and 8.8 ± 0.7 ng *S100A4* protein per 20 flies, respectively,
98 compared with undetectable levels (<0.1 ng) in parental controls
99 [Student *t* test (STT); $P = 0.29$]. Remaining details are in
100 Supplementary Methods. All initial *Drosophila* strains were
101 described previously (21), remaining details are in Supplemen-
102 tary Methods. The flies were maintained in standard yeast agar
103 medium at 25°C in a 12-hour light–dark incubator (21).

104 Metastatic assay

105 The *eyeless-FLP*-induced recombination of the *FRT*-flanked γ
106 linker in *Act>\gamma>GAL4* results in reconstitution of *Actin-GAL4* and
107 expression of *UAS-GFP*, and other *UAS* elements, in the develop-
108 ing eye (22). Dissemination of GFP from its original site of eye-
109 antennal discs to VNCs was scored for each genotype/experimen-
110 tal condition on a scale of 0 to 3 (16). GFP localized in the optic
111 lobes scored zero (stage 0), GFP on one side of the VNC scored 1
112 (stage I), on two sides of VNC scored 2 (stage II), and dissemina-
113 tion further into the VNC scored 3 (stage III). Average stage
114 score of metastasis (ASSM) ± SE was recorded for each genotype/
115 experimental condition. Fluorescent staining is described in Sup-
116 plementary Methods. Confocal images of GFP were captured (21)
117 and analyzed using ImageJ software (23), as described in Sup-
118 plementary Methods. Corrected integrated fluorescence intensity
119 (CIFI) = integrated intensity – (area of selected background
120 brain × mean fluorescence density of background) (23). Mean
121 CIFI ± SE was recorded.

122 Western blot analysis

123 This is described in Supplementary Methods. To correct for any
124 loading differences, original intensity of each band was divided by
125 that of actin. Intensity of each band for a particular larval group
126 was then expressed as a ratio of that in the *Ras^{Val12}* larvae. Mean
127 value of three experiments ± SE was recorded. To ensure the
128 intensity of band signals lay within the linear range, a plot of
129 band intensity against μg GAPDH was drawn ($y = 43947 \times$
130 -42398 , $r^2 = 0.997$) and band intensity for any protein outside
131 the linear range was excluded from the data and if necessary the gel
132 was rerun with higher or lower levels of total protein.

133 Drug treatment

134 Inhibitors, JNK-IN-8 (kindly provided by Nathanael S. Gray,
135 Harvard Medical School, Boston, MA; ref. 24) and batimastat (cat.
136 no.: SML0041; Sigma-Aldrich; ref. 25) were added directly from
137 1 mg/mL stock dissolved in DMSO to larval medium preheated to
138 55–60°C. Same concentration of DMSO was added to controls
139 without inhibitors. The drugs were incubated with the larvae
140 continuously until harvesting at the third instar stage, equivalent
141 to 7 days.

142 Statistical analyses

143 The significance of the difference between two categorical
144 groups for each genotype, those with and those without

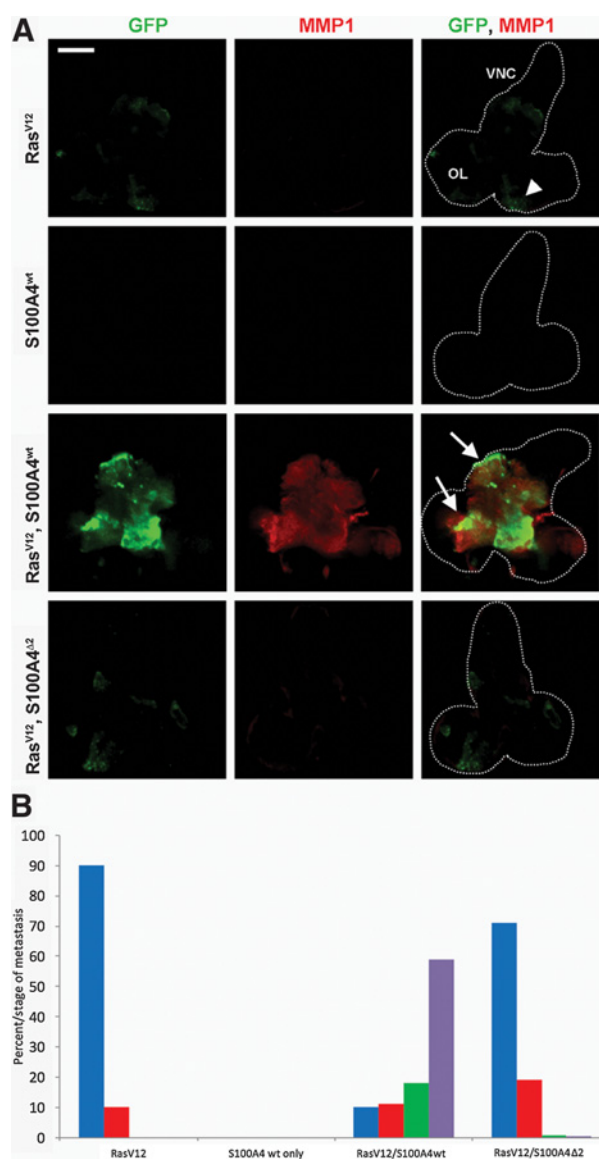


Figure 1.

A, Fluorescent images of GFP and MMP1 in larval CNS of different male recombinant *Drosophila*. CNS was dissected from third instar larvae of *Drosophila* with the following backgrounds: *Ras^{Val12}*(*RasV12*) only; *S100A4* wild type (*S100A4wt*) only; *Ras^{Val12}*, *S100A4* wild type (*RasV12/S100A4wt*); and *Ras^{Val12}*, *S100A4Δ2* (*RasV12/S100A4Δ2*). Representative CNS images show green fluorescence due to endogenous GFP, red fluorescence due to fluorescently labeled antibodies to matrix metalloproteinase1(MMP1), and merged fluorescent images are due to GFP and anti-MMP1. The outline of the relevant structures of the brain including optic lobes (OL) and ventral nerve cord (VNC) are indicated by the broken white line. The region which clearly expresses MMP in *Ras^{Val12}*, *S100A4* transgenics (arrows), and the same region in *Ras^{Val12}* transgenics (arrow head) are shown (Scale bar, 100 μm). **B**, Histogram of resultant recombinant larvae. The percentage (percent) larvae with different stages (0–III) of metastasis from the optic lobes to the ventral nerve cords (VNC) is shown for the recombinant *Drosophila*. The VNC of at least 50, third instar larvae were scored for the extent of metastasis on a sliding scale (Materials and Methods): from stage 0 (blue), stage I (red), stage II (green), and stage III (purple). Larvae containing *Ras^{Val12}/S100A4* were significantly different from those containing *Ras^{Val12}* alone, *S100A4* alone, and *Ras^{Val12}/S100A4Δ2* (Fisher exact test $P < 0.0001$) and between larvae containing *Ras^{Val12}* and *Ras^{Val12}/S100A4Δ2* ($P = 0.012$).

Q5

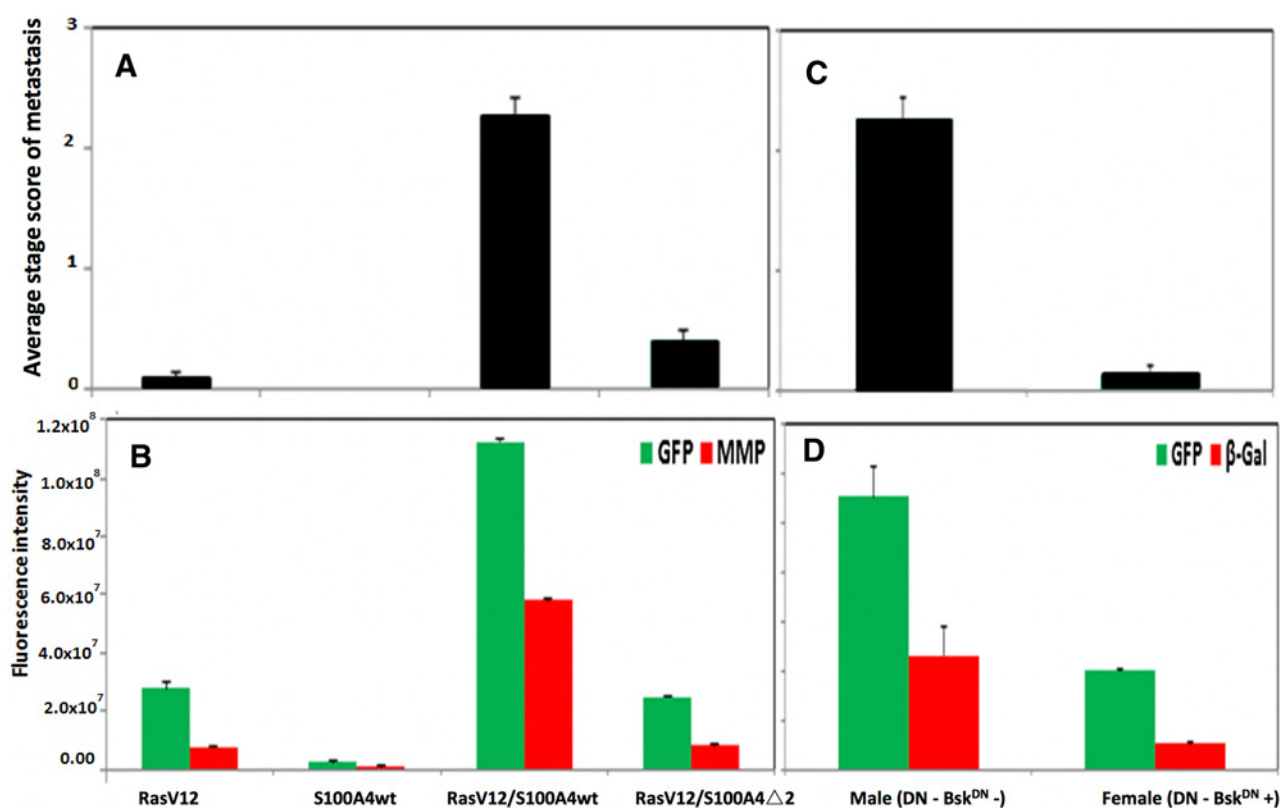


Figure 2.

Tumor dissemination in different recombinant *Drosophila* larvae. **A**, Average stage of metastatic spread in *Ras^{Val12}/S100A4* flies. ASSM of the primary tumor in the optic lobe spreading to the VNC is shown for male recombinant *Drosophila* with genetic backgrounds of: *Ras^{Val12}* (*RasV12*), *S100A4* wild type only (*S100A4wt*), *Ras^{Val12}* plus *S100A4* wild type (*RasV12/S100A4wt*), and *Ras^{Val12}* plus *S100A4mutantΔ2* (*RasV12/S100A4Δ2*). At least 50 larvae were scored (Materials and Methods) and results are expressed as mean ± SE. Both double transgenic flies were significantly different from flies with *Ras^{Val12}* genotype (STT.P ≤ 0.005) and *Ras^{Val12}/S100A4wt* from *Ras^{Val12}/S100A4Δ2* genotype (*P* = 0.0001). **B**, Fluorescence intensity of CNS images of *Ras^{Val12}/S100A4* flies. Endogenous fluorescence from GFP (green) and from exogenously-added labeled antibody to MMP1 (red) were recorded. CIFI of images of the dissected CNS from the same larvae in A were computed as described in "Methods." Mean ± SE is shown. For GFP green fluorescence, *Ras^{Val12}/S100A4wt* versus *Ras^{Val12}* only, *S100A4wt* only, or *Ras^{Val12}/S100A4Δ2* (STT.P < 0.0001); *Ras^{Val12}* vs. *Ras^{Val12}/S100A4Δ2* (*P* = 0.49). For MMP-1 red fluorescence, *Ras^{Val12}/S100A4wt* versus *Ras^{Val12}* only, *S100A4wt* only, and *Ras^{Val12}/S100A4Δ2* (STT.P < 0.0001); but *Ras^{Val12}* versus *Ras^{Val12}/S100A4Δ2* larval CNS (*P* = 0.15). **C**, Average stage of metastatic spread in male and female JNK-suppressed *Ras^{Val12}/S100A4* flies. ASSM of the primary tumor in the optic lobe spreading to the VNC is shown for recombinant *Drosophila* male and female larvae with the genetic backgrounds of *Ras^{Val12}/S100A4wt* in which the *Bsk^{DN}* dominant suppressor of JNK is expressed only in female flies. At least 20 larvae were scored as in **A**. Results are expressed as mean ± SE and there was a highly significant difference (STT.P < 0.0001). **D**, Quantification of the levels of fluorescent GFP and β-galactosidase in JNK suppressed flies. Endogenous fluorescence from GFP (green) and from exogenously-added labeled antibody to β-galactosidase (β-Gal) (red) were recorded. CIFI of images of the dissected CNS from the same larvae as in **C** were computed for male and female *Drosophila* with the *Ras^{Val12}/S100A4wt* genetic background. Mean ± SE is shown. The β-galactosidase is a marker of the activity of JNK (Materials and Methods). For GFP green fluorescence and β-galactosidase red fluorescence, significant reduction for female versus male *Ras^{Val12}/S100A4wt* larvae (STT.P < 0.0001 and *P* = 0.004, respectively).

147 metastases was determined by Fisher exact test, recording two-
 148 sided values of *P*. The significance of the difference in ASSM, in
 149 CIFI for GFP and MMP1, and in mean corrected intensity of each
 150 protein band in Western blots were calculated using two-sided
 151 Student *t* test (Stats Direct). Differences considered significant
 152 when *P* < 0.05.

153 Patients and specimens

154 A retrospective study was undertaken using samples of 183
 155 primary tumors from unselected breast cancer patients, as
 156 described previously (26, 27). Ethical approval was obtained
 157 from NRES Committee, North West REC.Ref. 12/NW/0778, Pro-
 158 tocol no. UoL000889, IRAS no. 107845. Samples were preserved

in neutral buffered-formalin and embedded in paraffin-wax, as
 described previously (7).

IHC staining

This is described in Supplementary Methods. Western blots of
 breast cell lines verified the specificity of all three mAbs to MMPs
 yielding apparent molecular weights of 73,99,75 kDa for secreted
 latent MMP2, 9, 13, respectively, consistent with those reported
 recently (28). Remainders were verified previously (27). IHC-
 stained sections were analyzed and scored (7, 26, 28, 29), as
 recorded in Supplementary Methods. Association of staining for
 MMP2, 9, and 13 with patient survival time is reported in
 Supplementary Methods.

174 **Results** 215
 175 **Cooperation of Ras^{Val12} and S100A4 in producing metastases in** 216
 176 **recombinant *Drosophila*** 217
 177 The brain containing the CNS was dissected from at least fifty, 218
 178 third instar larvae of different recombinant *Drosophila*. Male larvae 219
 179 with the genetic background *Ras^{Val12}* alone (*Ras^{Val12}* larvae) 220
 180 produced GFP-fluorescent tumors almost exclusively in the eye 221
 181 lobes (Fig. 1A) of 48 of 53 cases, with only 5 of 53 cases extending 222
 182 into one or the other side of the VNC (Fig. 1B). Extent of metastasis 223
 183 was semiquantified as described in Materials and Methods to 224
 184 produce an ASSM. There were no GFP-tumor deposits in the eye 225
 185 lobes or elsewhere in *S100A4* larvae (Figs. 1A and B and 2A). The 226
 186 *Ras^{Val12}/S100A4wt* recombinant larvae produced metastasis to the 227
 187 VNC (Fig. 1C) in a significantly higher number of 53 of 59 cases 228
 188 [Fisher exact test, *P* (FET.P) < 0.0001; Fig. 1B], increasing the ASSM 229
 189 by a significant 24-fold over *Ras^{Val12}* larvae [Student *t* test *P* (STT.P) 230
 190 < 0.0001; Fig. 2A]. There was also extensive metastasis to other 231
 191 organs, particularly to the gut and gonads (Supplementary Fig. 232
 192 S1). The *Ras^{Val12}/S100A4Δ2* inactive mutant larvae (Materials and 233
 193 Methods) produced a significantly lower number of 16 of 56 with 234
 194 metastasis to the VNC (FET.P < 0.0001; Fig. 1B), with significant 235
 195 5.7-fold reduction in ASSM compared to *Ras^{Val12}* larvae (STT.P = 236
 196 0.0001; Figs. 1A and 2A). The CIFI of GFP (Materials and Meth- 237
 197 ods) for images taken of the dissected CNS of *Ras^{Val12}* larvae 238
 198 was increased by a significant 4.1-fold in *Ras^{Val12}/S100A4wt* 239
 199 larvae (STT.P < 0.0001; Fig. 2B), but there was no significant 240
 200 difference in CIFI of *Ras^{Val12}/S100A4Δ2* mutant larvae compared 241
 201 with *Ras^{Val12}* larvae (STT.P = 0.49; Fig. 2B). 242
 202 **Quantification of Ras, GFP, and S100A4 levels by Western blot** 243
 203 **analysis** 244
 204 Antibodies to S100A4 detected a specific band of the correct 245
 205 apparent molecular weight of 9 kDa in all fly lines containing the 246
 206 *S100A4wt* or *S100A4Δ2* mutant gene, but no corresponding band 247
 207 in larvae containing *Ras^{Val12}* alone (Supplementary Fig. S2). 248
 208 Larvae containing the *Ras^{Val12}/S100A4wt* and *Ras^{Val12}/S100A4Δ2* 249
 209 genes produced a significant increase in Ras and a similar increase 250
 210 in GFP over that in larvae containing *Ras^{Val12}* alone (STT.P < 251
 211 0.001; Table 1). Protein bands of Ras and GFP were observed at 252
 212 the correct molecular weights (21 and 27 kDa, respectively; 253
 213 Supplementary Fig. S2 and Table 1). There was also highly 254

significant increases of 220 ± 5 - and 85 ± 11 -fold in S100A4 protein in larvae containing the *Ras^{Val12}/S100A4wt* and *Ras^{Val12}/S100A4Δ2* genes, respectively (*P* < 0.0001; Table 1), when normalized to GFP. Thus, there is a significant association of expression of active S100A4 and metastasis in this model system.

Increased levels of activated JNK and MMP1 in Ras and S100A4-overexpressing larvae

Levels of JNK in *Ras^{Val12}* and *Ras^{Val12}/S100A4wt* larvae were not significantly different in Western blots analysis (STT.P = 0.50; Table 1). However, levels of activated phospho-JNK and MMP1 at the reported molecular weights of 46 and 52 kDa, respectively (30), rose significantly by 13.1 ± 0.6 - and 3.8 ± 0.1 -fold, respectively, when normalized to GFP, in *Ras^{Val12}/S100A4wt* compared to *Ras^{Val12}* larvae (*P* < 0.0001; Supplementary Fig. S2 and Table 1). There was no significant increase in phospho-JNK, JNK, and MMP1 in *Ras^{Val12}/S100A4Δ2* compared to *Ras^{Val12}* larvae. In *S100A4wt* larvae alone, the levels of phospho-JNK, JNK, and MMP1 were significantly lower (*P* < 0.0001, *P* < 0.0001, *P* = 0.02; Supplementary Fig. S2 and Table 1), probably reflecting the absence of any primary tumor (Figs. 1A and B and 2A). There was also a modicum of red fluorescence for MMP1 in the eye lobes of *Ras^{Val12}* larvae (Fig. 1A and B), which rose significantly in *Ras^{Val12}/S100A4wt* larvae (*P* < 0.0001; Fig. 2B) showing extensive staining of the VNC (Fig. 1A and B). There was no significant difference in CIFI for *Ras^{Val12}* and *Ras^{Val12}/S100A4Δ2* larvae (Fig. 2B).

Activated JNK and MMP are downstream effectors in Ras and S100A4-overexpressing larvae

To determine the requirement for JNK signaling in the metastatic phenotypes, we expressed dominant-negative JNK encoded by *basket* (*Bsk^{DN}*), together with *Ras^{Val12}* and *S100A4*. When female and male siblings with and without *Bsk^{DN}*, respectively (Materials and Methods) were examined, 15/15 male, but only 2/15 female larvae produced extensive metastases to the VNC (FET.P < 0.0001; Supplementary Fig. S3). ASSM and CIFI were reduced by a significant 17- and 2.8-fold in female larvae, respectively (STT.P < 0.0001; Fig. 2C and D). The expression of a genetically-engineered marker of JNK activity, *puclacZ* was followed by its induction of β-galactosidase (Materials and Methods; Supplementary Fig. S3). The CIFI for red fluorescent antibody to β-galactosidase fell significantly by 4.7-fold in females (*P* = 0.004;

06 **Table 1.** Quantification of Western blots of different *Drosophila* lines

Antibody to ^a	Mean relative abundance ^b			
	Ras ^{Val12}	S100A4wt	Ras ^{Val12} /S100A4wt	Ras ^{Val12} /S100A4Δ2
(A) Ras	1 ± 0.05	0.0097 ± 0.001	3.56 ± 0.08 ^c	1.96 ± 0.16 ^c
(B) GFP	1 ± 0.04	0.011 ± 0.002	3.50 ± 0.05 ^c	1.60 ± 0.10 ^c
(C) S100A4	1 ± 0.06	9.62 ± 2.1	742 ± 19 ^d	136 ± 18 ^d
(D) P-JNK	1 ± 0.01	0.19 ± 0.02 ^e	40.5 ± 0.2 ^d	1.32 ± 0.08
(E) Total JNK	1 ± 0.04	0.23 ± 0.01 ^e	1.15 ± 0.07	1.04 ± 0.10
(F) MMP	1 ± 0.04	0.40 ± 0.07 ^f	13.1 ± 0.3	0.498 ± 0.001
MMP	1 ± 0.04	nd	2.17 ± 0.08 ^g	nd

Abbreviation: nd, not determined.

^aTen μg protein larval extracts were treated with the antibody shown in Western blots of Supplementary Fig. S2.

^bMean relative abundance after scanning the blots by densitometry (Materials and Methods) and the area under the peak corresponding to each protein was first normalized to that of actin and then ratioed to the level of that protein in the *Ras^{Val12}* male larvae which was arbitrarily set at 1. Mean relative abundance ± SE from three separate experiments.

^cStudent *t* test *P* < 0.001 over *Ras^{Val12}* male larvae.

^dStudent *t* test *P* < 0.0001 over *Ras^{Val12}* male larvae or *S100A4wt* male larvae.

^eStudent *t* test *P* < 0.0001 over *Ras^{Val12}* male larvae.

^fStudent *t* test *P* = 0.02 over *Ras^{Val12}* male larvae.

^gStudent *t* test *P* < 0.0001, for female over male larvae.

257 Supplementary Fig. S3 and Fig. 2D). In Western blots analysis, the
258 level of MMP1 protein normalized to that in male Ras^{Val12} larvae
259 fell 6.0-fold from 13.1 ± 0.3 to 2.17 ± 0.08 in male versus female
260 larvae ($P < 0.0001$; Table 1).

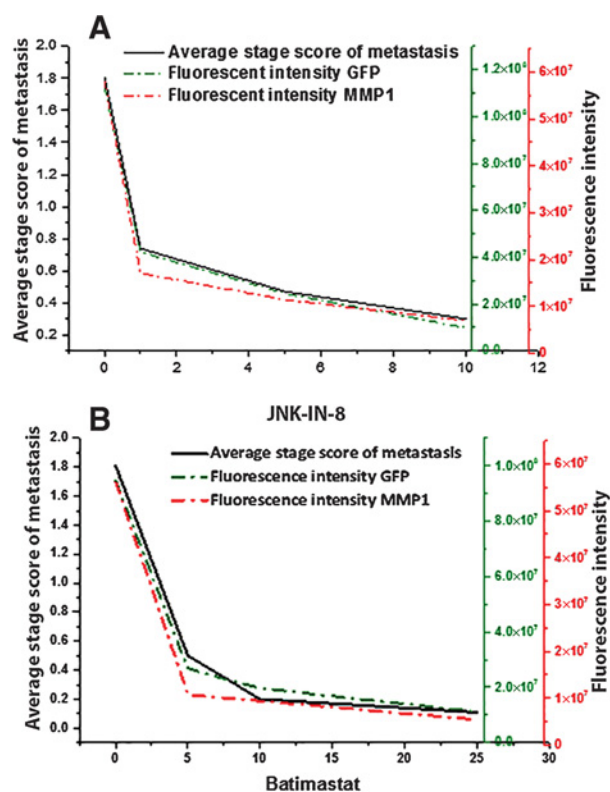
261 When increasing concentrations of the JNK-IN-8 inhibitor (24)
262 were added to male $Ras^{Val12}/S100A4wt$ larvae, there was a signifi-
263 cant fall in ASSM of 2.5-fold for 1 $\mu\text{mol/L}$ (STT.P < 0.0001), but
264 thereafter a more gradual stepwise decline; the overall fall being
265 5.8-fold ($P < 0.0001$; Supplementary Fig. S4A and S4B; Fig. 3A).
266 There was a similar significant decline in CIFI for GFP of 2.7-fold
267 ($P = 0.002$) for 1 $\mu\text{mol/L}$ inhibitor and then successive significant
268 decreases; the overall fall being 11.4-fold ($P < 0.0001$) (Fig. 3A).
269 There was also a similar significant decline in CIFI for antibodies
270 to endogenous MMP1 upon addition of 1 $\mu\text{mol/L}$ JNK-IN-8
271 (Supplementary Fig. S4A and S4B; $P = 0.0005$), then further
272 successive significant decreases; the overall fall being 8.3-fold
273 ($P < 0.0001$; Fig. 3A).

274 When increasing concentrations of the inhibitor of MMP activity,
275 Batimastat (25) was added to $Ras^{Val12}/S100A4wt$ larvae, there
276 were significant falls in ASSM of 3.4-fold for 5 $\mu\text{mol/L}$ ($P <$
277 0.0001), but thereafter the decline was more gradual; the overall
278 fall being 16.4-fold ($P < 0.0001$; Supplementary Fig. S4C and
279 S4D; Fig. 3B). There was a similar significant decline in CIFI for
280 GFP of 3.5-fold ($P = 0.0002$) for 5 $\mu\text{mol/L}$ inhibitor and then
281 successive nonsignificant decreases. The overall fall was 8.4-fold
282 ($P < 0.0001$; Fig. 3B). There was also a rapid significant decline
283 in CIFI for antibodies to endogenous MMP1 upon addition of
284 5 $\mu\text{mol/L}$ batimastat (Supplementary Fig. S4C and S4D) of 5.2-
285 fold ($P = 0.028$), then nonsignificant successive falls; the overall
286 fall being 10.3-fold ($P < 0.0001$; Fig. 3B). Thus, a definite pathway
287 has been established between S100A4 and MMP1 for induction of
288 metastasis in this model system.

289 Association of MMPs with patient survival time in human breast 290 cancer

291 Next, we investigated the relationship in human breast cancer
292 between the more commonly-occurring, mammalian MMPs,
293 MMP2, 9, 13, and patient demise as a result of metastatic cancer
294 (31). On examination of 183 breast carcinomas for IHC for these
295 three MMPs, 32% to 67% contained carcinoma cells which were
296 negatively stained (<1% carcinoma cells stained), 19% to 26%
297 were borderline stained (1–5% carcinoma cells stained), and the
298 rest (15–47%) were stained to varying degrees (Fig. 4 and Sup-
299 plementary Fig. S5; Supplementary Table S1). There were also
300 some reactive stromal cells, mainly myofibroblasts, macrophages,
301 and neutrophils which stained (Fig. 4). Assessment of staining
302 class was made only for the malignant cells. Staining for individ-
303 ual MMPs was abolished by prior incubation of each antibody
304 with the requisite MMP (Supplementary Fig. S5).

305 To determine whether there was any association between
306 staining for the separate MMPs and of survival of patients,
307 Kaplan–Meier survival curves were plotted for different staining
308 groups. Overall, there was a significant difference in staining for
309 each MMP (Wilcoxon Gehan Statistics, $P < 0.001$). However, the
310 largest significant differences occurred between the (±) and (+)
311 staining groups for MMP2, 9, and 13, respectively (Supplemen-
312 tary Table S2). The 183 patients were therefore separated into two
313 categorical groups using a cutoff of 5% stained carcinoma cells for
314 each MMP. Only $11 \pm 4\%$ survived with positively stained tumors,
315 compared to $81 \pm 4\%$ with negatively stained tumors
316 for MMP2; $10 \pm 6\%$ vs. $58 \pm 4\%$ for MMP9; and $22 \pm 5\%$ versus



317 **Figure 3.**

318 Tumor dissemination in recombinant flies treated with either JNK-IN-8 (A) or
319 Batimastat (B). *Drosophila* larvae with genetic background of $Ras^{Val12}/$
320 $S100A4wt$ were fed either (A) 0, 1, 5, or 10 $\mu\text{mol/L}$ of the JNK inhibitor JNK-IN-8
321 or (B) 0, 5, 10, or 25 $\mu\text{mol/L}$ of the MMP1 inhibitor Batimastat in their medium
322 (Materials and Methods). At least 20 larvae were scored and ASSM was
323 computed as described in Materials and Methods. These same larvae were
324 dissected, stained, and scored for endogenous green fluorescence from GFP and
325 for red fluorescence from exogenously-added labeled antibody to MMP1.
326 The CIFI was computed as described in Materials and Methods. Results are
327 shown as mean \pm SE. For ASSM, transgenic larvae fed 0 $\mu\text{mol/L}$ of inhibitor were
328 significantly higher than for larvae fed 1, 5, and 10 $\mu\text{mol/L}$ JNK-IN-8 or for larvae
329 fed 5, 10, and 25 $\mu\text{mol/L}$ batimastat (STT.P ≤ 0.0001). For JNK inhibitor-treated
330 larvae, decrease in CIFI for those fed 1, 5, and 10 $\mu\text{mol/L}$ JNK-IN-8 of 2.7, 4.6,
331 and 11.4 folds, respectively for GFP fluorescence (STT.P ≤ 0.002) and of 3.4, 5.1,
332 and 8.3 folds, respectively, for MMP1-related fluorescence (STT.P ≤ 0.0005). For
333 MMP1 inhibitor-treated larvae, decrease in CIFI for those fed on 5, 10, and
334 25 $\mu\text{mol/L}$ batimastat of 3.5, 4.8, and 8.4 folds, respectively, for GFP
335 fluorescence (STT.P ≤ 0.0002), and of 5.2, 5.9, and 10.3 folds, respectively, for
336 MMP1-related fluorescence (STT.P = 0.02, 0.07, and 0.06, respectively).

317 $75 \pm 5\%$ for MMP13 (Fig. 5). All differences were highly signifi-
318 cant ($P < 0.001$) with median duration of survival of 47, 32, and
319 52 months for MMP2, 9, and 13 positively stained tumors versus
320 228 months in all cases of negatively stained tumors. These
321 corresponded to relative risks (RR) of death of 9.04 (95% CI,
322 5.32–15.36), 4.69 (95% CI, 2.89–7.62), and 4.87 (95% CI, 2.98–
323 7.97), respectively. Results for S100A4 with a cutoff of 5% were
324 similar to that for individual MMPs with only $9 \pm 4\%$ surviving
325 versus $80 \pm 4\%$ for unstained tumors, median survival time of 46
326 months versus 228 months ($\chi^2 = 71.8$, $P < 0.001$), and RR of
327 patient death of 9.96 (95% CI, 5.87–16.9; Supplementary Table
328 S3). Patients with tumors stained positively for all three MMPs
329 showed no significant increase in mortality (7% \pm 6%), decrease
330

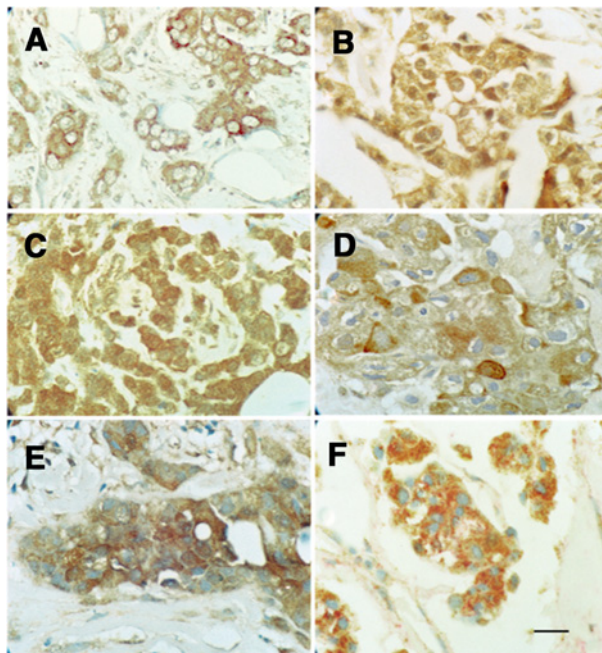


Figure 4. Immunohistochemical staining of different breast carcinomas with antibody to MMP2 (A), MMP9 (B), or MMP13 (C) showing strong brown staining of the carcinoma cells' cytoplasm. Incubation with antibody to S100A4 (D) or S100P (E) showing strong, bead-like, cytoplasmic staining. F, Incubation with antibody to MMP2 with brown chromophore and to S100A4 with red chromophore showing most carcinoma cells were stained by both antibodies. Tumors were selected to show strong staining in A to C for their respective MMP, but the same tumor was stained in D to F as in A ($\times 180$; scale bar, 20 μm).

333 in median survival time (30 months), or increase in RR (4.96; 95%
 334 CI, 2.99–8.24) than staining for either MMP2 or MMP9 separately
 335 (Supplementary Table S2). When all three MMPs were included in
 336 Cox's multivariate regression analysis (Materials and Methods),
 337 the individual contributions made to the time of patient demise
 338 showed that staining for MMP2 ($P < 0.001$) and that for MMP9
 339 ($P = 0.025$) were independently significant while that for MMP13
 340 was not (Supplementary Table S3).

341 **Association of MMPs with S100A4 and patient survival**

342 Results for IHC staining for the 3 MMPs using a 5% cutoff were
 343 cross-tabulated against pathologic variables and IHC staining for
 344 S100A4, S100P (29), estrogen receptor α (ER α), progesterone
 345 receptor (PgR), c-erbB-2 (Her2), cytokeratin 5/6 (CK5/6), and
 346 CK14 (32). All these variables have been reported to influence
 347 survival times in the same set of patients (26). Positive staining for
 348 each of MMP2, 9, and 13 was associated strongly with positive
 349 staining for S100A4 when using a 5% cutoff for S100A4. This
 350 association was slightly reduced with staining for S100P using a
 351 5% cutoff (Table 2). Significance of association was much more
 352 marked for staining for S100A4 than for S100P when using a 1%
 353 cutoff. There was also a significant association with staining for
 354 CK5/6 and usually for CK14 (Table 2). Positive staining for any
 355 MMP was not significantly associated with involved lymph nodes,
 356 high tumor grade, large tumor size, nor with positive staining for
 357 ER α , PgR, or c-erbB-2 (Table 2). There was also a highly significant
 358 association of staining for each pair of MMPs (Table 2 and
 359 Supplementary Table S4).

When staining for S100A4 was tested for its relative probability
 of association (RA) with that for the three MMPs using binary
 logistic regression, that with MMP2 was strongest at 4.21 ($P <$
 0.001), that with MMP9 of 2.41 was not significant, and that with
 MMP13 of 2.17 ($P = 0.051$) was very nearly significant. When
 staining for each of the MMPs, in turn, was assessed with staining
 for S100A4, CK14, ER α , PgR, and c-erb-2, only that for S100A4
 and partially that for CK14 proved to be significant (Supplementary
 Table S5). When repeated using a different cutoff for S100A4
 (1% instead of 5%; Table 2) and additionally including that for
 S100P, staining for MMP2 was most closely associated with that
 for S100A4 (Supplementary Table S5). To determine whether the
 three MMPs were independent of S100A4 when related to patient
 survival, they were included in a series of Cox's multivariate
 regression analyses (Materials and Methods; Supplementary
 Table S3). When a single MMP and S100A4 were only included,
 staining for S100A4 always emerged as the most significant
 association with patient survival time. Similar results were
 obtained if staining for S100A4 and all three MMPs were included
 in the same analysis, S100A4 emerged as the most significant
 association followed by MMP2 and then MMP9, whereas that due
 to MMP13 was not significant (Supplementary Table S3).

To determine whether there was coexpression of the MMPs and
 S100 proteins, two breast carcinomas were chosen that were either
 moderately or strongly stained for MMP2, and these were IHC
 retained for S100A4/P, 3 MMPs, CK5/6, and CK14. Exactly the
 same areas were examined for each antigen. The percentage of
 stained cells for S100A4 was not significantly different from that
 for MMP2 and MMP13, while staining for S100P was not signifi-
 cantly different from that for MMP9 (Supplementary Fig. S6; and
 Supplementary Table S6). Staining for S100A4 or MMP2 was also
 not significantly different from that for CK5/6, but only in the
 MMP2 moderately-stained carcinomas; all the other paired combi-
 nations were significantly different (Supplementary Fig. S6; and
 Supplementary Table S6). When serial sections from three breast
 carcinomas strongly-staining for MMP2 were doubly IHC-stained
 for S100A4 with red and for MMP2 with brown chromophores on
 the same section, there were (mean \pm SE) 80.2 \pm 2.2% doubly
 stained cells, 6.9% \pm 0.9% cells stained red for S100A4, 2.9% \pm
 0.4% cells stained brown for MMP2 and 9.1% \pm 1.5% unstained
 cells (ANOVA, $F = 669.3$, 3 df, $P < 0.001$; Supplementary Fig. S7).
 Thus, S100A4 is associated with and partially confounded for
 patient survival by the three MMPs to varying degrees.

Discussion

We have shown for the first time that S100A4 can induce
 metastasis in the *Drosophila* model and that the oncogene *Ras^{Val12}*
 largely fails in this respect. The increase in number of larvae
 bearing VNC metastases (10-fold), in ASSM (24-fold), and in
 CIFI (4.1-fold) for *Ras^{Val12}/S100A4* over *Ras^{Val12}* larvae demon-
 strates clearly that S100A4 promotes extensive dissemination
 to the VNC, as well as elsewhere in the larvae (Supplementary
 Fig. S1). The reason for the differences in fold increases is due to
 the method of measurement, the CIFI included GFP fluorescence
 due to the primary as well as the metastases, whereas the first
 two parameters relate only to the metastases. That larvae contain-
 ing *Ras^{Val12}* and inactive *S100A4 Δ 2* genes (20) show significantly
 less metastases (Fig. 1A, 2A, and B), demonstrates that the
 migratory/invasive ability of S100A4 (20) is required for its
 metastatic ability. That *S100A4* larvae produce no tumors at all

361
 362
 363
 364
 365
 366
 367
 368
 369
 370
 371
 372
 373
 374
 375
 376
 377
 378
 379
 380
 381
 382
 383
 384
 385
 386
 387
 388
 389
 390
 391
 392
 393
 394
 395
 396
 397
 398
 399
 400
 401
 402
 403
 404
 405
 406
 407
 408
 409
 410
 411
 412
 413
 414
 415
 416
 417
 418
 419

Figure 5. Association of immunohistochemical staining for MMPs with overall time of patient survival. Cumulative proportion of surviving patients as a fraction of the total for each year after presentation for patients with carcinomas classified as negatively-stained (set a, solid line) or positively-stained (set b, dotted line) is shown for MMP2 (A), MMP9 (B), and MMP13 (C). Numbers of patients entering each year are shown below. The two curves are highly significantly different in each case (Wilcoxon statistic $\chi^2 = 71.81, 32.50, \text{ or } 41.90$ for A, B, or C, respectively, 1 df, $P < 0.001$). Further details are shown in Supplementary Materials.

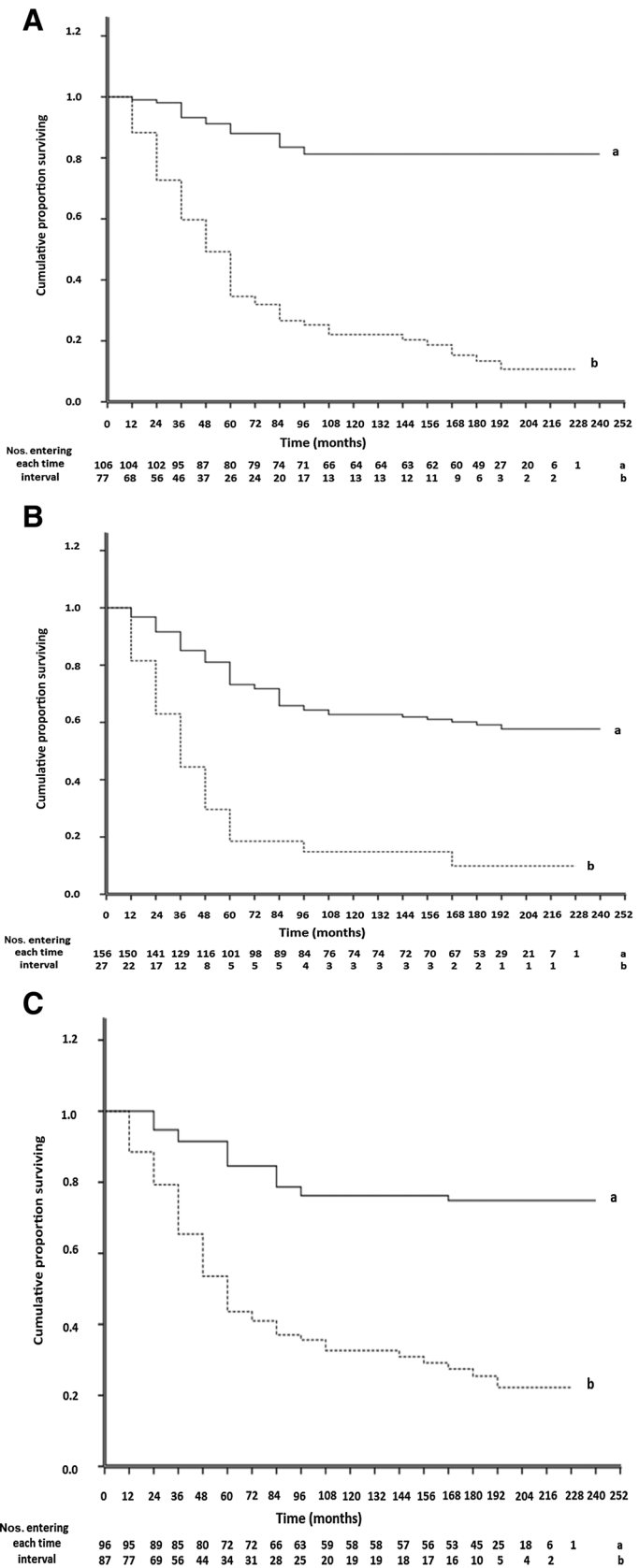


Table 2. Association of IHC staining for MMPs with other tumor variables

Tumor variable ^a	Patient ^b no.	Statistical significance ^c		
		MMP2	MMP9	MMP13
Lymph nodes	139	0.271	0.564	0.681
Grade	164	0.997	0.656	0.156
Tumor size	177	0.467	0.937	0.985
MMP2	183	—	9.0×10^{-7}	1.7×10^{-12}
MMP9	183	9.0×10^{-7}	—	1.2×10^{-7}
MMP13	183	1.7×10^{-12}	1.2×10^{-7}	—
S100A4 (5%)	183	6.6×10^{-9}	2.9×10^{-4}	2.4×10^{-6}
S100A4 (1%)	183	0 ^d	1.2×10^{-7}	1.9×10^{-8}
S100P (5%)	163	2.3×10^{-7}	2.2×10^{-3}	1.3×10^{-7}
S100P (1%)	163	1.6×10^{-4}	0.012	2.4×10^{-5}
CK14	172	5.7×10^{-7}	2.8×10^{-3}	0.372
CK5/6	173	1.6×10^{-6}	0.035	5.6×10^{-3}
ER α	181	1.00	1.0	1.0
PgR	172	0.995	0.983	0.549
C-erbB-2	183	0.660	1.00	0.809

^aLymph nodes with or without tumor deposits; grade, histologic grades I and II vs. grade III; tumor size <5 cm vs. >5 cm in diameter; presence or absence of IHC staining for molecular variables using 5% cutoff for MMP2, MMP9, MMP13, S100A4 (5%), S100P (5%), ER α , PgR, c-erbB-2, and using a 1% cutoff for S100A4 (1%), S100P (1%), CK14, and CK5/6.

^bNumber of patients from original 183.

^cProbability *P* from Fisher exact test using the Holm-Bonferroni correction calculated as $1 - (1 - P)^n$, where $n = 12$ (Materials and Methods).

^dUncorrected $P = 7.7 \times 10^{-18}$.

(Fig. 1A, 2A, and B) demonstrates that *S100A4* alone is non-oncogenic, consistent with previous results in our *S100A4* transgenic mice (33). The increases in Ras and GFP proteins of 3.5- to 4-fold (Table 1) are consistent with the increase in GFP fluorescence of about 4-fold (Fig. 2B) and probably represent the increase in overall tumor mass between the *Ras^{Val12}* and the *Ras^{Val12}/S100A4* larvae.

In agreement with different genetically manipulated *Ras* oncogenic systems in *Drosophila* (16, 18), the levels of endogenous activated phospho-JNK and MMP1 rise significantly in *Ras^{Val12}/S100A4* compared with *Ras^{Val12}* larvae (Table 1). The rise in MMP1 protein is of the same order as the increase in fluorescently-labeled antibodies to MMP1. That JNK is indeed a downstream effector of *Ras^{Val12}/S100A4* for metastasis is demonstrated by the reduction in the number with metastases and their ASSM in female *Bsk^{DN}*-expressing larvae compared to the male un-suppressed larvae (Fig. 2C). That these suppressed values for *Ras^{Val12}/S100A4* are not significantly different from those of the *Ras^{Val12}* larvae (Fig. 2C) suggests that the predominant driver of the JNK-link to metastasis is the overexpression of S100A4. The 4.7-fold fall in the immunofluorescently-detectable β -galactosidase in the female, suppressed *Ras^{Val12}/S100A4* larvae demonstrates that JNK needs to be activated to stimulate metastasis. Because of the level of JNK protein is relatively constant between *Ras^{Val12}* and *Ras^{Val12}/S100A4* larvae (Table 1), S100A4 probably triggers activation of JNK by stimulating its increase in phosphorylation (24). Results using 10 μ mol/L JNK-IN-8 confirm that JNK-induced phosphorylation of c-Jun is a necessary step in the S100A4-triggered pathway for metastasis. That there is a fall in CIFI for immunofluorescently detectable MMP1 (Fig. 3B) positions JNK before MMP in any pathway (16). Moreover, the fact that the MMP1 inhibitor, batimastat (25) inhibits ASSM and CIFI for GFP in the *Ras^{Val12}/S100A4* larvae places MMP1 on the direct pathway to metastasis. The order of this novel S100A4-induced metastatic pathway is: S100A4 \rightarrow phospho-JNK \rightarrow c-Jun \rightarrow MMP1 \rightarrow metastasis. Thus, S100A4 appears to replicate the loss of function of suppressor genes *scrib* and *lethal2* (17) or *Her2* activation in the JNK/MMP pathway (16, 18). In transgenic mice or chemically transformed rat mammary cells, S100A4 combines with oncogenic *Neu* (*Her2*;

ref. 6) or *Ras* (4), respectively to stimulate, via the cytoskeleton, cell migration, and then subsequent events for invasion/metastasis (34). However, the involvement of this novel pathway has hitherto been unreported.

The relevance of our unique *Drosophila* model for S100A4 has been pursued in human breast cancer. IHC staining of our cohort of 183 breast carcinomas for the individual MMPs2, 9, 13 demonstrates 15% to 47% primary tumors are stained positively using a cut-off of 5%, in approximate agreement with previous reports (35, 36). Here we show that the overall duration of survival of patients with positively-stained carcinomas is highly significantly worse than for those patients classified as not staining for one of MMP2, 9, or 13 (Fig. 5), in agreement with results for MMP2 in hepatocarcinoma (37), skin melanoma (38) and for MMP13 in breast (36) and colon cancer (39). In contrast, MMP9 has been reported to be a favorable indicator in lymph-node-negative breast cancer (40). This favorable prognosis may depend on the much higher cutoff employed, because of our node-negative group showed no significant difference (Wilcoxon $\chi^2 = 2.63$, 1 df, $P = 0.11$). This difference was significantly greater for MMP9 staining in our node-positive patients ($\chi^2 = 18.40$, 1 df, $P < 0.001$). The other two MMPs showed similar significant differences in node-negative and node-positive patients (MMP2 $\chi^2 = 25.46$ and 25.39; MMP13 $\chi^2 = 14.91$ and 12.93, respectively). These results may suggest that MMP9 operates later than the other two MMPs at a post lymph-node-spreading stage in the disease process.

Overall, the RR of patient death in separate univariate analyses is greatest for patients with tumors stained for S100A4 (9.96), followed closely by those stained for MMP2 (9.04), then for MMP13 (4.87), and finally for MMP9 (4.69; Supplementary Table S3). However, the antibodies used here to detect the MMPs do not discriminate between inactive precursors or cleaved active MMPs and do not detect inhibitory TIMPs (41). Usually in cultured cells, S100A4 increases expression of MMP precursors and this results in an enhanced proteolytic activity and cell invasion/metastasis (42, 43). Moreover, S100A4 can act both intracellularly (43, 44) and extracellularly via RAGE receptors (45, 46) to stimulate MMP production. The fact that *Bsk^{DN}* inhibits S100A4-induced MMP1

503 and metastasis to the VNC in our *Drosophila* model (Fig. 2C and D) 547
 504 suggests that MMP1 is produced by the tumor cells and not by 548
 505 reactive stromal cells (47), consistent with immunohistochemical 549
 506 results in our human breast cancers. In contrast to the *Drosophila* 550
 507 model, the three JNK proteins in human cancers can exert both 551
 508 pro- and anti-oncogenic effects depending on the cell type and 552
 509 cross-talk with other kinases (48, 49). Thus, the oncogenic effect 553
 510 of activated JNK cannot be determined in human cancers from the 554
 511 measurement of its level alone, and hence was not attempted here. 555
 512 Upon manipulation in cultured cells, S100A4 has been 556
 513 reported to control production of a single MMP, one of MMP2, 557
 514 9, or 13, depending on the source and sometimes the report (42– 558
 515 45). In contrast, we show here that positive staining for each 559
 516 MMP2, 9, or 13 is separately and in combination very strongly 560
 517 associated with S100A4 and to a lesser extent with S100P (Table 561
 518 2). The significant association of staining for MMP2, 9 with the 562
 519 basal cell markers CK5/6, CK14 has been reported previously 563
 520 (50), predominantly placing these MMPs, together with S100A4 564
 521 and S100P, in the most aggressive subtype of breast cancers (26). 565
 522 When tested for RA of staining for S100A4 with the other three 566
 523 MMPs together, S100A4 is more likely to occur with MMP2, and 567
 524 the higher significant RA of MMP2 for S100A4 over a combination 568
 525 of other proteins confirms this result (Supplementary Table S6). 569
 526 Thus, S100A4 is more associated with MMP2, 13, and S100P more 570
 527 with MMP9, at least at the cellular level (Supplementary Table S6). 571
 528 This differential association in the tumor raises the novel possi- 572
 529 bility of synergistic interactions between the S100 proteins (29) 573
 530 occurring via different target MMPs. 574
 531 Multiple longitudinal comparisons with survival time for all 575
 532 three MMPs together in multivariate analysis shows that only 576
 533 MMP2 and MMP9 are independently significant, whereas the 577
 534 contribution of MMP13 is confounded by that due to the other 578
 535 two MMPs (Supplementary Table S3). These results suggest partial 579
 536 overlap occurs between MMP2/MMP9-related pathways and 580
 537 MMP13-related pathways, whereas those related to MMP2 and 581
 538 MMP9 are more separate. This result is consistent with their 582
 539 function, MMP13 is a collagenase which is required to cut col- 583
 540 lagen fibrils first, before the two gelatinases, MMP2 or MMP9, can 584
 541 digest the remainder (51). When S100A4 and each MMP are tested 585
 542 in combination, the order of reduction in RR for S100A4 is MMP2
 543 (42% reduction), then MMP13 (27% reduction) and finally
 544 MMP9 (11% reduction), whereas the reduction in RR for each
 545 MMP separately with S100A4 is similar (44%, 40%, and 43%,
 respectively; Supplementary Table S3). These results suggest the
 pathways that S100A4 may trigger leading to premature death
 from metastatic disease overlap, to some extent, with those
 triggered by the three MMPs, the most overlap being with
 MMP2-related and then with MMP13-related pathways. The
 results for the close association of S100A4 and MMP2 are con-
 firmed at the level of the cell where 91% of S100A4-containing
 cells also contain MMP2 and 96% of MMP2-containing cells also
 contain S100A4 (Supplementary Fig. S7). The considerable
 enhancing effect of S100P on S100A4-linked patient demise
 (29) may then be attributable, at least in part, to S100P targeting
 different MMPs from those targeted by S100A4 (Supplementary
 Table S6). This differential targeting of MMPs by S100 proteins is a
 novel mechanism for generation of the known synergy between
 different MIPs in the development of many cancers.

Disclosure of Potential Conflicts of Interest

No potential conflicts of interest were disclosed.

Authors' Contributions

Conception and design: T.M. Ismail, D. Bennett, R. Barraclough, P.S. Rudland
Development of methodology: T.M. Ismail, D. Bennett, A.M. Platt-Higgins, P.S. Rudland
Acquisition of data (provided animals, acquired and managed patients, provided facilities, etc.): T.M. Ismail, D. Bennett, P.S. Rudland
Analysis and interpretation of data (e.g., statistical analysis, biostatistics, computational analysis): T.M. Ismail, D. Bennett, A.M. Platt-Higgins, M. Al-Medhity, P.S. Rudland
Writing, review, and/or revision of the manuscript: T.M. Ismail, D. Bennett, A.M. Platt-Higgins, M. Al-Medhity, R. Barraclough, P.S. Rudland
Administrative, technical, or material support (i.e., reporting or organizing data, constructing databases): T.M. Ismail, A.M. Platt-Higgins, P.S. Rudland
Study supervision: T.M. Ismail, P.S. Rudland

Grant Support

This work was supported by Cancer and Polio Research Fund (to T.M. Ismail, A.M. Platt-Higgins, M. Al-Medhity, R. Barraclough, P.S. Rudland) and Medical Research Council G0801447 (to A.M. Platt-Higgins, R. Barraclough, P.S. Rudland), and MR/K015931/1 (to D. Bennett).

The costs of publication of this article were defrayed in part by the payment of page charges. This article must therefore be hereby marked *advertisement* in accordance with 18 U.S.C. Section 1734 solely to indicate this fact.

Received June 30, 2016; revised October 19, 2016; accepted October 27, 2016; published OnlineFirst xx xx, xxxx.

58:Q11

References

- Dunnington DJ, Hughes C, Monaghan P, Rudland PS. Phenotypic instability of rat mammary tumor epithelial cells. *J Natl Cancer Inst* 1983;71:1227–40.
- Dunnington DJ, Kim U, Hughes CM, Monaghan P, Ormerod EJ, Rudland PS. Loss of myoepithelial cell characteristics in metastasizing rat mammary tumors relative to their nonmetastasizing counterparts. *J Natl Cancer Inst* 1984;72:455–66.
- Steeg PS. Tumour metastasis: mechanistic insights and clinical challenges. *Nat Med* 2006;12:895–904.
- Davies BR, Davies MP, Gibbs FE, Barraclough R, Rudland PS. Induction of the metastatic phenotype by transfection of a benign rat mammary epithelial cell line with the gene for p9ka, a rat calcium-binding protein, but not with the oncogene EJ-ras-1. *Oncogene* 1993;82:99–1008.
- Barraclough R, Savin J, Dube SK, Rudland PS. Molecular cloning and sequence of the gene for p9ka. A cultured myoepithelial cell protein with strong homology to S-100, a calcium-binding protein. *J Mol Biol* 1987;198:13–20.
- Davies MP, Rudland PS, Robertson L, Parry EW, Jolicœur P, Barraclough R, et al. Expression of the calcium-binding protein S100A4 (p9ka) in MMTV-neu transgenic mice induces metastasis of mammary tumours. *Oncogene* 1996;13:1631–7.
- Rudland PS, Platt-Higgins A, Renshaw C, West CR, Winstanley JH, Robertson L, et al. Prognostic significance of the metastasis-inducing protein S100A4 (p9ka) in human breast cancer. *Cancer Res* 2000;60:1595–603.
- Mazzucchelli L. Protein S100A4: too long overlooked by pathologists? *Am J Pathol* 2002;160:7–13.
- Jenkinson SR, Barraclough R, West CR, Rudland PS. S100A4 regulates cell motility and invasion in an in vitro model for breast cancer metastasis. *Br J Cancer* 2004;90:253–62.
- Gross SR, Sin CG, Barraclough R, Rudland PS. Joining S100 proteins and migration: for better or for worse, in sickness and in health. *Cell Mol Life Sci* 2014;71:1551–79.
- Bazigou E, Apitz H, Johansson J, Loren CE, Hirst EM, Chen P-L, et al. Anterograde Jelly belly and Alk receptor tyrosine kinase signalling mediate retinal axon targeting in *Drosophila*. *Cell* 2007;128:961–75.
- Halder G, Callaerts P, Flister S, Walldorf U, Kloter U, Gehring WJ. Eyeless initiates the expression of both sine oculis and eyes absent

- 628 during *Drosophila* compound eye development. *Development* 1998;125:2181–91. 691
- 629 13. Hauck B, Gehring W, Walldorf U. Functional analysis of an eye specific 692
- 630 enhancer of the eyeless gene in *Drosophila*. *Proc Natl Acad Sci U S A* 693
- 631 1999;96:564–9. 694
- 632 14. Belvin MP, Anderson KV. A conserved signalling pathway: the *Drosophila* 695
- 633 toll-dorsal pathway. *Ann Rev Cell Biol* 1996;12:393–416. 696
- 634 15. Bennett D, Lyulcheva E, Cobbe N. *Drosophila* as a potential model for ocular 697
- 635 tumours. *Ocul Oncol Pathol* 2015;1:190–9. 698
- 636 16. Uhlirva M, Bohmann D. JNK- and FOS-regulated Mmp1 expression 699
- 637 cooperates with Ras to induce invasive tumours in *Drosophila*. *EMBO J* 700
- 638 2006;25:5294–304. 701
- 639 17. Brumby AM, Richardson HE. Scribble mutants cooperate with oncogenic 702
- 640 Ras or Notch to cause neoplastic overgrowth in *Drosophila*. *EMBO J* 703
- 641 2003;22:5769–79. 704
- 642 18. Duffy JB. GAL4 system in *Drosophila*. A fly geneticist's Swiss army knife. 705
- 643 *Genesis* 2002;34:1–15. 706
- 644 19. Evans PC, Smith TS, Lai MJ, Williams MG, Burke DF, et al. A novel type of 707
- 645 deubiquitinating enzyme. *J Biol Chem* 2003;278:23180–6. 708
- 646 20. Ismail TM, Fernig DG, Rudland PS, Terry CJ, Wang G, et al. The basic C- 709
- 647 terminal amino acids of calcium-binding protein S100A4 promote metas- 710
- 648 tasis. *Carcinogenesis* 2008;29:2259–66. 711
- 649 21. Ciurciu A, Duncalf L, Jonchere V, Lansdale N, Vasieva O, Glenday P, et al. 712
- 650 PNuTs/PP1 regulates RNAPII-mediated gene expression and is necessary 713
- 651 for developmental growth. *PLOS Genetics* 2013;9:e1003885. 714
- 652 22. Baranski TJ, Cagan RL inventor; Washington University, assignee. Trans- 715
- 653^{Q12}genic *Drosophila* and methods of use thereof. WO2009055461A1. 2009 Apr 716
- 654 30. 717
- 655 23. McCloy RA, Rogers S, Caldon CE, Lorca T, Castro A, Burgess A, et al. Partial 718
- 656 inhibition of cdk1 in G2 phase overrides the SAC and decouples mitotic 719
- 657 events. *Cell Cycle* 2014;13:1400–12. 720
- 658 24. Zhang T, Inesta-Vaquera F, Niepel M, Zhang J, Ficarro SB, Machleidt T, et al. 721
- 659 Discovery of selective covalent inhibitions of JNK. *Chem Biol* 2012;19: 722
- 660 140–54. 723
- 661 25. Sledge GW Jr, Qulai M, Goulet R, Bone EA, Fife R. Effect of matrix 724
- 662 metalloproteinase inhibitor batimastat on breast cancer regrowth and 725
- 663 metastasis in athymic mice. *J Natl Cancer Inst* 1995;87:1546–50. 726
- 664 26. de Silva Rudland S, Platt-Higgins A, Winstanley JHR, Jones NJ, Barraclough 727
- 665 R, West CR, et al. Statistical association of basal cell keratins with metas- 728
- 666 tasis-inducing proteins in a prognostically unfavorable group of sporadic 729
- 667 breast cancers. *Am J Pathol* 2011;79:1061–72. 730
- 668 27. Rudland PS, Platt-Higgins A, Davies LM, de Silva Rudland S, Wilson JB, 731
- 669 Aladwani A, et al. Significance of the Fanconi anemia FANCD2 protein in 732
- 670 sporadic and metastatic human breast cancer. *Am J Pathol* 2010;176: 733
- 671 2935–47. 734
- 672 28. Orgaz JL, Pandya P, Dalmeida R, Karagiannis P, Sanchez-Loorden B. 735
- 673 Diverse matrix metalloproteinase functions regulate cancer amoeboid 736
- 674 migration. *Nat Commun* 2015;5:4255–70. 737
- 675 29. Wang G, Platt-Higgins A, Carrol J, de Silva Rudland S, Winstanley J, 738
- 676 Barraclough R, et al. Induction of metastasis by S100P in a rat mammary 739
- 677 model and its association with poor survival of breast cancer patients. 740
- 678 *Cancer Res* 2006;66:1199–207. 741
- 679 30. Glasheen BM, Kabra AT, Page-McCaw A. Distinct functions for the catalytic 742
- 680 and hemopexin domains of *Drosophila* matrix metalloproteinase. *Proc Natl* 743
- 681 *Acad Sci U S A* 2009;106:2659–64. 744
- 682 31. Verma RP, Hansch C. Matrix metalloproteinases (MMPs): chemical-bio- 745
- 683 logical functions and (Q) SARs. *Bioorg Med Chem* 2007;15:2223–68. 746
- 684 32. Sorlie T, Tibshirani R, Parker J, Hastie T, Marron JS, Nobel A, et al. Repeated 747
- 685 observation of breast tumor subtypes in independent gene expression data 748
- 686 sets. *Proc Natl Acad Sci U S A* 2003;100:8418–23. 749
- 687 33. Davies M, Harris S, Rudland PS, Barraclough R. Expression of the rat, S-100- 750
- 688 related, calcium-binding protein gene, p9Ka, in transgenic mice demon- 751
- 689 strates different patterns of expression between these two species. *DNA Cell* 752
- 690 *Biol* 1995;14:825–32. 691
- 692 34. Du M, Wang G, Ismail TM, Gross S, Fernig DG, Barraclough R, et al. 693
- 694 S100P dissociates myosin IIA filaments and focal adhesion sites to 695
- 696 reduce cell adhesion and enhance cell migration. *J Biol Chem* 2012;287: 697
- 698 15330–44. 699
- 699 35. Hao X, Sun B, Hu L, Lahdesmaki H, Dunmire V, Feng Y, et al. Differential 700
- 701 gene and protein expression in primary breast malignancies and their 702
- 702 lymph node metastases as revealed by combined cDNA microarray and 703
- 703 tissue microarray analysis. *Cancer* 2004;100:1110–22. 704
- 704 36. Zhang B, Cao X, Liu Y, Cao W, Zhang F, Zhang S, et al. Tumour-derived 705
- 705 matrix metalloproteinase-13 (MMP13) correlations with prognosis. *BMC* 706
- 706 *Cancer* 2008;8:183–84. 707
- 707 37. Sze KM, Wong KL, Chu GK, Lee JM, Yau TO, Ng OP-L, et al. Loss of 708
- 708 phosphatase and tensin homolog enhances cell invasion and migration 709
- 709 through AKT/Sp-1 transcription factor/matrix metalloproteinase 2 activa- 710
- 710 tion in hepatocellular carcinoma and has clinicopathologic significance. 711
- 711 *Hepatology* 2011;53:1558–69. 712
- 712 38. Rotte A, Martinka M, Li G. MMP2 expression is a prognostic marker for 713
- 713 primary melanoma patients. *Cell Oncol* 2012;35:207–16. 714
- 714 39. Yang B, Gao J, Rao Z, Shen Q. Clinicopathological significance and 715
- 715 prognostic value of MMP-13 expression in colorectal cancer. *Scand J Clin* 716
- 716 *Lab Invest* 2012;72:501–5. 717
- 717 40. Scorilas A, Karameris A, Arnoyiannaki N, Ardanavis A, Bassilopoulos P, 718
- 718 Trangas T, et al. Overexpression of matrix-metalloproteinase-9 in human 719
- 719 breast cancer: a potential favourable indicator in node-negative patients. *Br* 720
- 720 *J Cancer* 2001;84:1488–96. 721
- 721 41. Deryugina EI, Quingley JP. Matrix metalloproteinases and tumour metas- 722
- 722 tasis. *Cancer Metastasis Rev* 2006;25:9–34. 723
- 723 42. Schmidt-Hansen B, Klingelhofer J, Grum-Schwensen B, Christensen A, 724
- 724 Andresen S, Kruse C, et al. Functional significance of metastasis-inducing 725
- 725 S100A4 (Mts1) in tumor-stroma interplay. *J Biol Chem* 2004;279:24498– 726
- 726 504. 727
- 727 43. Zhang J, Zhang DL, Jiao XL, Dong Q. S100A4 regulates migration and 728
- 728 invasion in hepatocellular carcinoma HepG2 cells via NF- κ B-dependant 729
- 729 MMP-9 signal. *Eur Rev Med Pharmacol Sci* 2013;17:2372–82. 730
- 730 44. Jia W, Gao XJ, Zhang ZD, Yang ZX, Zhang G. S100A4 silencing suppresses 731
- 731 proliferation, angiogenesis and invasion of thyroid cancer cells through 732
- 732 downregulation of MMP-9 and VEGF. *Eur Rev Med Pharmacol Sci* 733
- 733 2013;17:1495–508. 734
- 734 45. Yammani RR, Carlson CS, Bresnick AR, Loeser RF. Increase in production of 735
- 735 matrix metalloproteinase 13 by human articular chondrocytes due to 736
- 736 stimulation with S100A4: role of the receptor for advanced glycation end 737
- 737 products. *Arthritis Rheum* 2006;54:2901–11. 738
- 738 46. Schmidt-Hansen B, Ornäs D, Crigorian M, Klingelhöfer J, Tulchinsky E, 739
- 739 Lukanidin E, et al. Extracellular S100A4(mts1) stimulates invasive growth 740
- 740 of mouse endothelial cells and modulates MMP-13 matrix metalloprotei- 741
- 741 nase activity. *Oncogene* 2004;23:5487–95. 742
- 742 47. Heppner KJ, Matrisian LM, Jensen RA, Rodgers WH. Expression of most 743
- 743 metalloproteinase family members in breast cancer represents a tumor- 744
- 744 induced host response. *Am J Pathol* 1996;149:273–82. 745
- 745 48. Wagner EF, Nebreda AR. Signal integration by JNK and p38 MAPK path- 746
- 746 ways in cancer development. *Nat Rev Cancer* 2009;9:537–49. 747
- 747 49. Cellurale C, Gimuis N, Jiang F, Cavanagh-Kyros J, Lu S, Garlick DS, et al. 748
- 748 Role of JNK in mammary gland development and breast cancer. *Cancer Res* 749
- 749 2012;72:472–81. 750
- 750 50. Radenkovic S, Konjevic G, Jurisic V, Karadzic K, Nikitovic M, Gopcevic K, 751
- 751 et al. Values of MMP-2 and MMP-9 in tumour tissue of basal-like breast 752
- 752 cancer patients. *Cell Biochem Biophys* 2014;68:143–52. 691
- 753 51. Sela-Passwell N, Rosenblum G, Shoham T, Sagi I. Structural and functional 692
- 754 bases for allosteric control of MMP activities: can it pave the path for 693
- 755 selective inhibition? *Biochim Biophys Acta* 2010;1803:29–38. 694
- 756 695
- 757 696
- 758 697
- 759 698
- 760 699
- 761 700
- 762 701
- 763 702
- 764 703
- 765 704
- 766 705
- 767 706
- 768 707
- 769 708
- 770 709
- 771 710
- 772 711
- 773 712
- 774 713
- 775 714
- 776 715
- 777 716
- 778 717
- 779 718
- 780 719
- 781 720
- 782 721
- 783 722
- 784 723
- 785 724
- 786 725
- 787 726
- 788 727
- 789 728
- 790 729
- 791 730
- 792 731
- 793 732
- 794 733
- 795 734
- 796 735
- 797 736
- 798 737
- 799 738
- 800 739
- 801 740
- 802 741
- 803 742
- 804 743
- 805 744
- 806 745
- 807 746
- 808 747
- 809 748
- 810 749
- 811 750
- 812 751
- 813 752

AUTHOR QUERIES

AUTHOR PLEASE ANSWER ALL QUERIES

- Q1: Page: 1: AU: Per journal style, genes, alleles, loci, and oncogenes are italicized; proteins are roman. Please check throughout to see that the words are styled correctly. AACR journals have developed explicit instructions about reporting results from experiments involving the use of animal models as well as the use of approved gene and protein nomenclature at their first mention in the manuscript. Please review the instructions at <http://www.aacrjournals.org/site/InstrAuthors/ifora.xhtml#genomen> to ensure that your article is in compliance. If your article is not in compliance, please make the appropriate changes in your proof.
- Q2: Page: 1: Author: Please verify the drug names and their dosages used in the article.
- Q3: Page: 1: Author: Please verify the affiliations and their corresponding author links.
- Q4: Page: 1: Author: Please verify the corresponding author details.
- Q5: Page: 2: Author: Please confirm quality/labeling of all images included within this article. Thank you.
- Q6: Page: 4: Author: Please verify the layout of Tables 1 and 2 for correctness.
- Q7: Page: 5: Author: Units of measurement have been changed here and elsewhere in the text from "M" to "mol/L," and related units, such as "mmol/L" and " μ mol/L," in figures, legends, and tables in accordance with journal style, derived from the Council of Science Editors Manual for Authors, Editors, and Publishers and the Système international d'unités. Please note if these changes are not acceptable or appropriate in this instance.
- Q8: Page: 9: AU/PE: The conflict-of-interest disclosure statement that appears in the proof incorporates the information from forms completed and signed off on by each individual author. No factual changes can be made to disclosure information at the proof stage. However, typographical errors or misspelling of author names should be noted on the proof and will be corrected before publication. Please note if any such errors need to be corrected. Is the disclosure statement correct?
- Q9: Page: 9: Author: The contribution(s) of each author are listed in the proof under the heading "Authors' Contributions." These contributions are derived from forms completed and signed off on by each individual author. As the corresponding author, you are permitted to make changes to your own contributions. However, because all authors submit their contributions individually, you are not permitted to make changes in the contributions listed for any other authors. If you feel strongly that an error is being made, then you may ask the author or authors in question to contact us about making the changes. Please note, however, that the manuscript would be held from further processing until this issue is resolved.
- Q10: Page: 9: Author: Please verify the heading "Grant Support" and its content for correctness.

Q11: Page: 9: Author: Ref. 7 has been updated as per PubMed. Please verify.

Q12: Page: 10: Author: Please verify Ref. 22 as typeset for correctness.

AU: Below is a summary of the name segmentation for the authors according to our records. The First Name and the Surname data will be provided to PubMed when the article is indexed for searching. Please check each name carefully and verify that the First Name and Surname are correct. If a name is not segmented correctly, please write the correct First Name and Surname on this page and return it with your proofs. If no changes are made to this list, we will assume that the names are segmented correctly, and the names will be indexed as is by PubMed and other indexing services.

First Name	Surname
Thamir M.	Ismail
Daimark	Bennett
Angela M.	Platt-Higgins
Morteta	Al-Medhity
Roger	Barraclough
Philip S.	Rudland